

THE AERODYNAMIC ANALYSIS OF THE PROFILES FOR FLYING WINGS

Vasile PRISACARIU

Transylvania University, Brasov, Romania

The possibility of using an un-piloted aerial vector is determined by the aerodynamic characteristics and performances. The design for a tailless unmanned aerial vehicles starts from defining the aerial vector mission and implies a series of geometrical and aerodynamic aspects for stability. This article proposes to remark the aerodynamic characteristics of three profiles used at flying wing airship through 2D software analysis.

Key words: *airfoil, flying wing, aerodynamic analysis, Reynolds number*

1. INTRODUCTION

The vector from the robotized aerial system acts the same as piloted airships having the same aerodynamic laws. While projecting a lift surface type flying wing an important aspect would be maneuverability and stability which is directly influenced by geometrical characteristics used in the designing phase.

Normally airships type flying wing could have lift surfaces with any aerodynamic profile, everything else depending on the type of mission and the performance of the bearing surface. To design such an airship at a large operating scale, the wing must present optimal geometrical characteristics so it can maintain induced resistance, the moment coefficient and the lift coefficient at suitable levels. A few aerodynamic profiles used at tailless airships are represented in **Figure 1**.

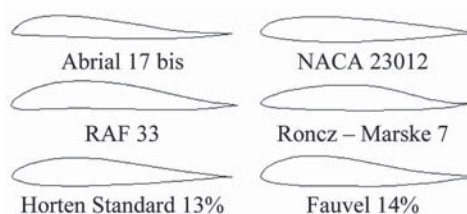


Figure 1 Airfoils for flying wing

The majority of the aerial vectors for the fixed wing have a conventional geometry with the tail, the low cost design determining to create a tailless project that has a blended wing or not, see figure 2. [1]

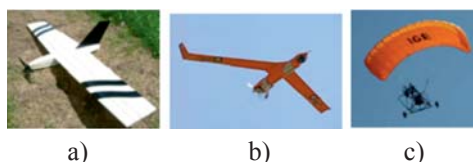


Figure 2. Flying wing UAV.
(a. Model free plan, b. Scan Eagle, USA, c. Maxi 10, France)

Mainly there are 3 types of flying wings determined by obtaining longitudinal stabilization: plank (fig. 2a), swept (fig. 2b) and parafoil (fig. 2c).

By choosing one of the longitudinal stabilizations we use a series of aerodynamic profiles corresponding to the momentary coefficient (low values), as examples we choose Phoenix and Clark YH profiles for plank and swept wings and MH 91 for parafoil wings (see figure 3)[2, 3].

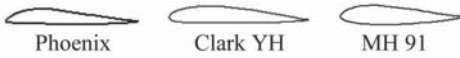


Figure 3. Airfoil for flying wing

2. THEORETICAL LANDMARKS

Aerodynamic analysis for airfoil reveals limits of performances can be obtained: the angle of incidence for zero lift (α_0), the angle of the incidence for zero drag $(C_d)_{\min}$, maximum smoothness $(C_d/C_l)_{\min}$ (figure 4), the angle of incidence at maximum lift – $(C_l)_{\max}$. [4]. Incidence reference values are shown in Figure 5.

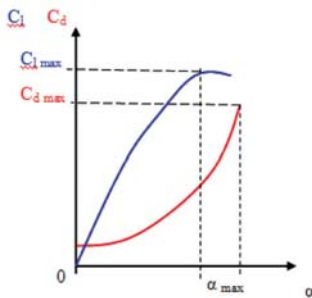


Figure 4. Dependence of lift coefficient (Cl) and drag coefficient (Cd) with angle of incidence (α)

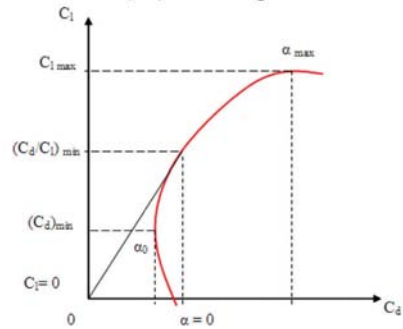


Figure 5. The classic polar

For performances calculus is necessary an explicit dependence of $C_d = C_d(C_l)$. Show in figure 4 a linear variation of C_l small incidence angles above 7° but the variation is nonlinear because of the separation of fluid layers. We have:

$$C_d = C_d(a, M, Re), C_l = C_l(a, M, Re) \quad (1)$$

removed α , result:

$$C_l = C_l(C_d, M, R) \quad (2)$$

Variation of the coefficients is show in figure 5 with M and Re known and constant, where: M – *nr. Mach*, Re – *nr. Reynolds*

$$c_l = \frac{L}{\frac{1}{2} \rho v_\infty^2 c b} \quad (3)$$

$$c_d = \frac{D}{\frac{1}{2} \rho v_\infty^2 c b} \quad (4)$$

$$c_{m_0} = \frac{M_0}{\frac{1}{2} \rho v_\infty^2 c^2 b} \quad (5)$$

where: L -*lift*, D -*drag*, M_0 -*aerodynamic moment*, b -*span*, c -*wing chord*.

3. AERODYNAMIC ANALYSIS

3.1. Profili v.2.2.1 software

For the 2D analysis we choose the profiles from figure 6 which are mainly used in building tailless aerial vectors, the analysis being performed by Profili 2.2.1 software [5] using the data from table 1.

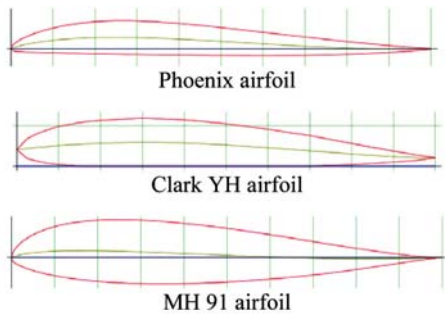


Figure 6. Airfoils

The analysis methodology for comparative graphics is described in the diagram in figure 7.

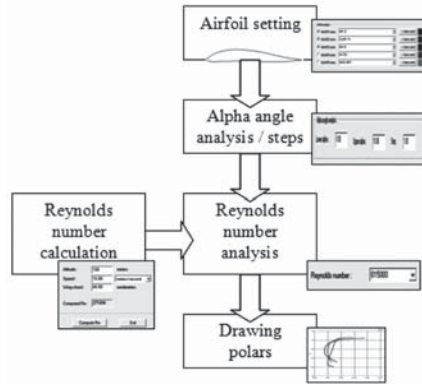


Figure 7. Analysis methodology [5]

Table 1. The conditions of the analysis

Features	Value		
CMA(mm)	400		
Flight height (m)	100		
Angle of incidence (0)	- 5 ÷ 15		
Speed (m/s)	10	20	30
Reynolds number Re	272000	543000	815000

For speed of 10 m/s ($R_e = 272000$) the polars of three airfoils are shown in figure 8 (a, b, c).

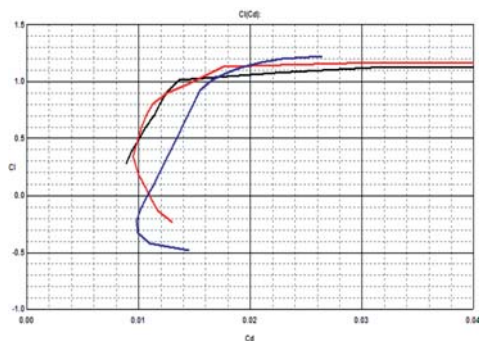


Figure 8 a. Chart Cl-Cd

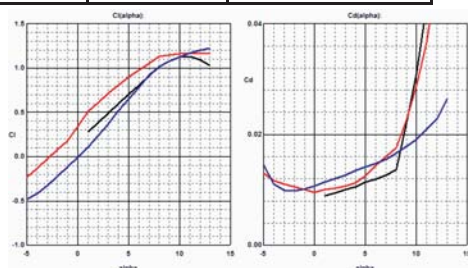


Figure 8b. Charts Cl - angle of the incidence, Cd - angle of incidence

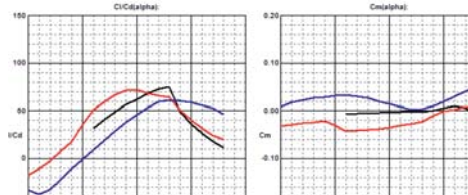


Figure 8c. Chart Cl/Cd - angle of the incidence, Cm - angle of incidence

The characteristics the three profiles are shown in table 2. [5, 6].

Table 2. Airfoil features

Features	Phoenix	Clark YH	MH 91
Thickness:	8,2%	11,9%	15%
Camber:	2,8%	6%	1,7%
Max C_{p_i} :	1,17	1,11	1,11
Max C_L angle:	11	15	15
Max L/D:	92,61	32,83	20,09
Max L/D angle:	7	4,5	3
Zero lift angle	-0,69	-2	0

We can see in the graphs (figure 9) pressure coefficient variation (C_p) reported at airfoil chord depending angle of incidence (α) at $Re = 272000$ for minimum speed of 36 km/h. We observe pressure coefficient (C_p) that is influenced by camber.

Analysis of the airfoil, made at $Re = 272,000$, in the case the curvature changes (flaps out at 5° and 10°) to 20% of chord, show increasing lift coefficient (C_l) and change the value of the moment coefficient (C_m), as graphs in figure 10 (a, b), figure 11 (a, b), figure 12 (a, b).

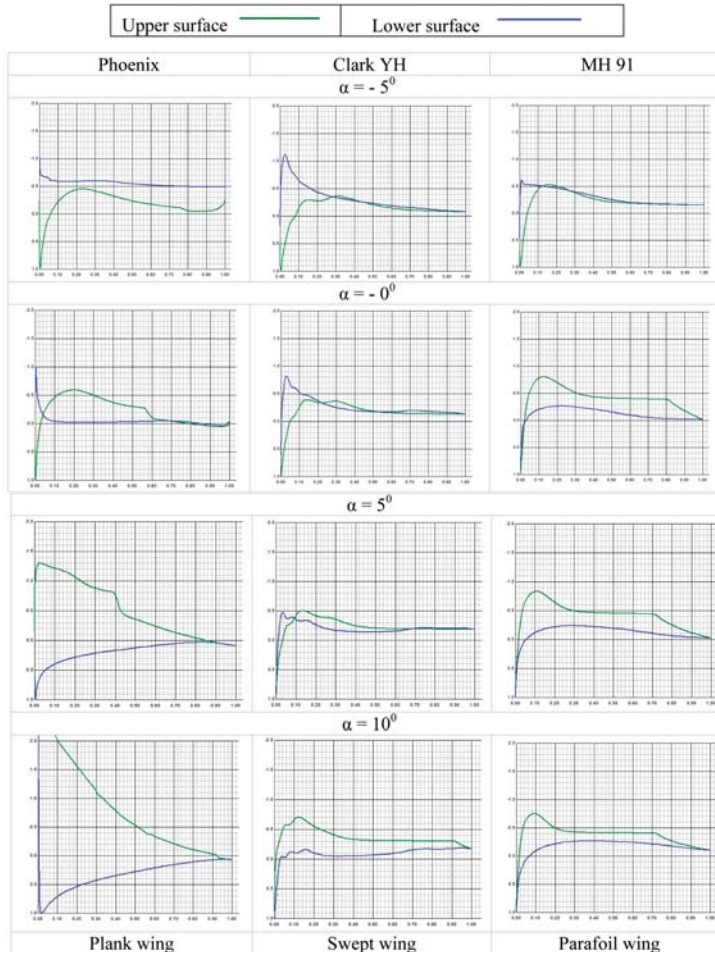


Figure 9. The variation pressure coefficient (C_p) compared to airfoil chord

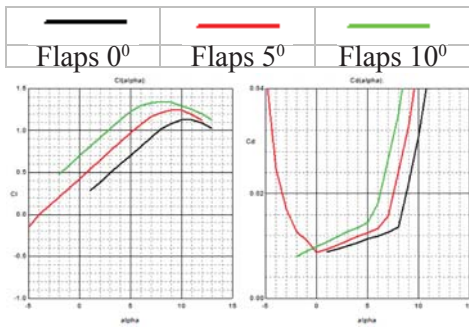


Figure 10 a. Phoenix airfoil, the charts Cl – angle of incidence, Cd – angle of incidence

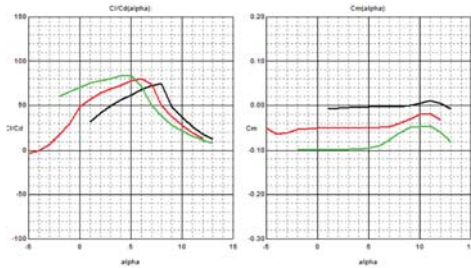


Figure 10 b. Phoenix airfoil, the charts Cl/Cd – angle of incidence, Cm – angle of incidence

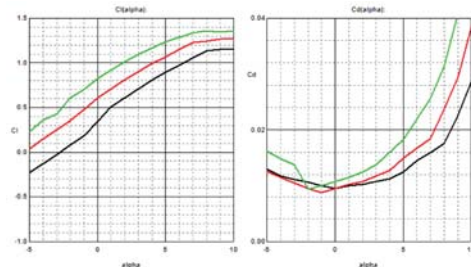


Figure 11 a. Clark YH airfoil, the charts Cl – angle of incidence, Cd – angle of incidence

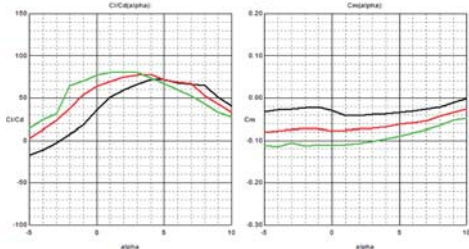


Figure 11 b. Clark YH airfoil, the charts Cl/Cd-angle of incidence, Cm – angle of incidence

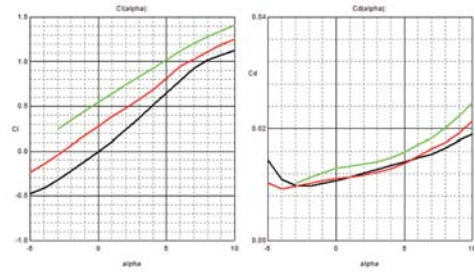


Figure 12 a. MH 91 airfoil, the charts Cl – angle of incidence, Cd – angle of incidence

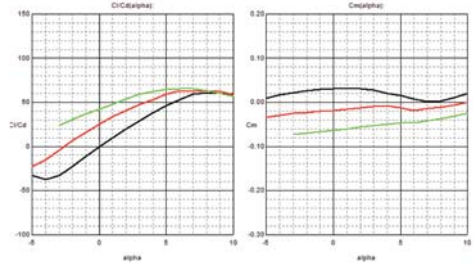


Figure 12 b. MH 91 airfoil, the charts Cl/Cd – angle of incidence, Cm – angle of incidence

3.2. Easy CFD v.4.1

It is a calculation instrument used for the fluid dynamic based on the numerical solutions of the fluids and heat transmission in Cartesian coordinates systems. We present the analysis with EASY CFD_G v.4.1 which is realized according to the methodology from figure 13 and the data from table 4 so we can find out the pressure coefficient that is around the three profiles which are subjected to laminar stream.

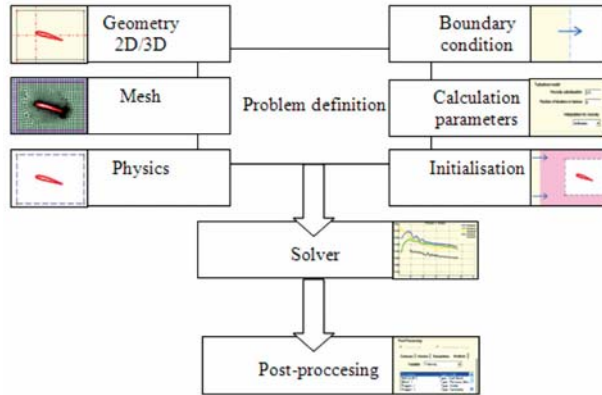


Figure 13. Analysis methodology

Table 3. Analysis data

Meshing	unstructured
Mesh spacing method	uniform
Mesh elements (max)	3000
Regime	steady-state
Thermal effects	isothermal
Iteration	100
Airfoil incidence	0°

The speed and pressure prints are remarked in figure 14. The validation of the analysis presented in Easy CFD_G v.4.1 could be start ups for deeper studies with refinements for the initial entry conditions for flow and advection models.

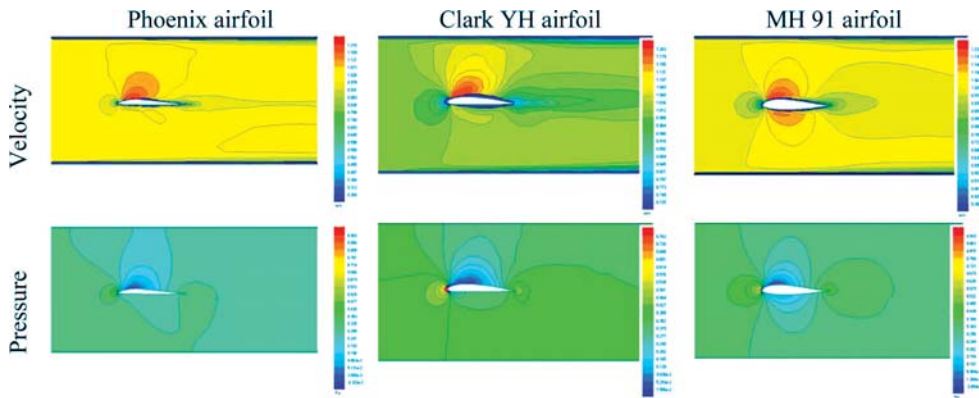


Figure 14. Easy CFD analysis.

Limits and options of the software

Profili 2.2.1 offers an aerodynamic analysis with a series of instruments and criteria which lead to a high trusted result. The most important analysis instruments are: profile manager (with a data base that contains 2000 profiles), Reynolds calculator (rope functions, speed and altitude), polar analysis profiles, speed and relevant analysis coefficients for profile flow (pressure, friction).

EASY CFD_G v.4.1 is simple software, mainly oriented for educational purpose becoming a valorous instrument for a first analysis. It presents a few options and characteristics which recommend him: laminar or turbulent flow, isothermal or non-isothermal flow, steady-state or transient flow, structured and unstructured mesh generation, two turbulence models, conduction in solid and conjugate heat transfer, multi component fluid flow, transport of passive scalars (smoke), geometry import from DXF or point data files [7].

4. CONCLUSIONS

By choosing one of the versions, stabilization for the flying wing is realized with the help of an auto-stabilized profile with negative geometrical torsion of the wings extremities and placing the gravity center under the pressure center of the lift surface. An important aspect is the speed and pressure distribution

for small Reynolds numbers which can lead to instability. The best compromise for a UAV flying wings is to adapt curved moderate line of the profile with a maxim curve moved to the leading edge [8].

Recent research with the help of the software led to the design of new profiles with multiple applications without too much experimental effort. The applications in unmanned aerial vehicles request abnormal qualities that are not met at piloted airships: maneuverability at small speeds and high overload.

ACKNOWLEDGMENT

The authors wish to thank the Transilvania University of Brasov and “Henri Coandă” Air Force Academy of Brasov for supporting the research necessary for writing this article.

REFERENCES

- [1] UAS Yearbook, *Unmanned aircraft systems – The Global Perspective 2011/2012*, Blyenburg & Co, June 2011, Paris, ISSN 1967-1709, p. 216
- [2] Airfoils database, www.airfoiltools.com, Available at 10.12.2012
- [3] Airfoils, ww.aerodesign.de/english/profile/profile_s.htm, Available at 10.12.2012
- [4] Deliu Ghe., *Mecanica aeronavelor*, Editura Albastră, 2001, Cluj-Napoca, ISBN 973-650-029-2, p. 375

[5] Duranti S. *Profili 2.21 software*, 2012, Feltre-Italia, www.profil2.com, Available at 12.12.2012

[6] Airfoil tools, www.worldofkrauss.com, Available at 14.12.2012

[7] Gameiro Lopes A.M., *Easy CFD_G user manual*, 2012, p. 98

[8] Airfoils for tailless airplanes, http://www.mh-aerotools.de/airfoils/nf_1.htm, Available at 18.01.2013